

Robustness of the pumping charge to dynamic disorder

R. Wang, and Z. Song*

School of Physics, Nankai University, Tianjin 300071, China

We investigate the effect of disorder on a gapped crystalline system by introducing a class of local quantities for an energy band, which is referred as to band correlation function (BCF) and is the sum of correlation functions for all eigenstates of the band. We show that the BCFs are robust in the presence of disorder if the band gap is not collapse. The eigenstate set of an energy band can be almost completely mapped onto the perturbed eigenstate set, referred as to quasi-closed mapping, when it is sufficiently isolated from other bands. Some features relate to translational symmetry may emerge in a randomly perturbed system. We demonstrate this by simulating numerically the pumping process for a 1D Rice-Mele (RM) model with disorders on the hopping strength and on-site potential. It is shown that the quantized pumping charge is robust against with the dynamic disorder. This result indicates the possibility of measuring the topological invariant in experimental system with imperfection.

I. INTRODUCTION

The notions of topology have been invoked in condensed matter physics and material sciences since the connection of integer quantum Hall conductances with topological Chern invariants was discovered¹. Topological theory has been well established in condensed matter physics²⁻²⁸. So far, the topological feature in matter is mainly described by topological invariant, Chern number, which greatly expands our knowledge on state of matters. It has explicit definition for crystalline system, in which the momentum is a crucial quantity, and thus the translational symmetry is necessary. On the other hand, it is usually claimed that the topological property is robust against disorder perturbations. This can be manifested in a rigorous manner by the existence of edge states of the system immune in the presence of disorder. The robustness of topological edge states has been actively explored in a wide variety of quantum Hall systems, topological insulators, and topological superconductors^{12,15}. A natural question thus arises as to whether the topological feature is insensitive to disorder in an approximate manner. It is a different and less explored subject but has potential applications in realistic systems. For instance, a Hall conductivity, that is related to the first Chern number for perfect topological system, appears as approximate integer in the presence of imperfection. Recently, some pertinent theoretical effort has been devoted to the topological phases in noncrystalline lattices²⁹⁻³¹.

In this work, we study the influence of disorder perturbation on the topological properties of a crystalline system. We show that there exist global quantities which remain unchanged under the disorder perturbation if the energy gap is not collapsed. It provides a unified framework to discuss topological invariant for disorder-perturbed system, such as Rice-Mele (RM) model with random distribution of hopping strength and on-site potential. We focus on a similar concept with Hall conductance in 2D topological system, the Thouless pumping charge^{32,33}. It is a local quantity, which can be mea-

sured without the need of translational symmetry. To demonstrate this point, we study a quasi-adiabatic process by numerical simulation. We implement the dynamic disorder by discretized time evolution under a sequence of Hamiltonians based on a set of time-dependent random numbers. Both the analytical analysis and numerical simulation show that pumping charge, as a measurable Chern number, is robust against the disorder. Our work provides a way of extracting topological invariant from an imperfect system.

This paper is organized as follows. In section II, we present the concept of quasi-closed mapping and the related application. In section III, we investigate the connection between the crystalline and noncrystalline RM models analytically and numerically. In section IV, we present the numerical results about the pumping charge in the presence of disorder. Section V summarizes the results and explores its implications.

II. ROBUSTNESS OF BAND CORRELATION FUNCTION

The concept of energy band originates from the periodic potentials is always associated with translational symmetry. However, a slight disorder perturbation may hybridize the energy levels but cannot destroy the density of states and collapse the energy gap. In this section, we investigate what remains of the energy band in the presence of disorder. We consider a generic Hamiltonian

$$H = \sum_{i,j=1}^N \gamma_{ij} c_i^\dagger c_j + \text{H.c.}, \quad (1)$$

which describes fermions hop from one site to another with amplitude γ_{ij} , and the on-site energy γ_{ii} . Here c_i^\dagger denotes fermion operator. We start with the case with

$$H = H_0 + H', \quad (2)$$

where H_0 has translational symmetry. For simplicity, we assume that there are two energy bands, with the

single-particle eigenstate set $\{|\psi_k^\sigma\rangle\}$ with $\sigma = \pm$ and $k \in [1, N/2]$. Here k labels the energy levels with wave vector (k_x, k_y, k_z) if a 3D system is considered. Obviously we have $\langle\psi_k^+|\psi_{k'}^-\rangle = 0$. When a small randomly perturbation H' is induced, the eigenstates set becomes $\{|\phi_n^\sigma\rangle\}$ with $\sigma = \pm$ and $n \in [1, N/2]$. For sufficient small perturbation, we always have $\langle\psi_k^\sigma|\phi_n^{-\sigma}\rangle \approx 0$, which is simple but crucial to this work. In a disordered system, $\{\gamma_{ij}\}$ becomes a set of random numbers around the $\{\gamma_{ij}^0\}$ of H_0 . In the large limit of disorder, the energy gap collapses and $\langle\psi_k^\sigma|\phi_n^{-\sigma}\rangle$ cannot be neglected. Fig. 1 schematically illustrates this point.

In the case that the perturbation does not collapse the original energy band, state $|\phi_n^\sigma\rangle$ is only the superposition of the sub-set $\{|\psi_k^\sigma\rangle\}$ approximately. In the following we focus on a single band and neglect the band index σ . For an arbitrary operator \mathcal{O} , the matrix representation with $\{|\psi_k\rangle\}$ is a $\langle\psi_k|\mathcal{O}|\psi_{k'}\rangle$. For a perturbed system, the matrix representation of \mathcal{O} changes but leaves the trace of the matrix unchanged approximately. Actually, the quasi-closed mapping admits

$$|\phi_n\rangle = \sum_k c_n^k |\psi_k\rangle, \quad (3)$$

where $c_n^k = \langle\psi_k|\phi_n\rangle$, satisfying $\sum_k c_n^k (c_n^k)^* = \delta_{nn'}$ and $\sum_n c_n^k (c_n^{k'})^* = \delta_{kk'}$. Then we have

$$\sum_n \langle\phi_n|\mathcal{O}|\phi_n\rangle = \sum_k \langle\psi_k|\mathcal{O}|\psi_k\rangle. \quad (4)$$

In physics, we are interested in the quantity

$$C_{i,j} = \sum_n \langle\phi_n|c_i^\dagger c_j|\phi_n\rangle, \quad (5)$$

which is termed as band correlation function (BCF) and has evident physical significance. For example, $C_{j,j}$ relates to particle density at j site. We know that $C_{j,j}$ for H_0 is identical when j belongs to a sublattice due to the translational symmetry, but it is a little surprisingly that this feature still holds when a slight randomly perturbation is added although the translational symmetry is broken. On the other hand, a BCF characterizes the feature of the band, probably involving the topology of the band.

III. DISORDERED RM MODEL

As an example, we consider a RM model with a time-dependent random perturbation on a $2N$ -site lattice. It provides a natural platform for studying topological invariant directly through dynamics both in theoretical^{34–36} and experimental³⁷ perspectives. The

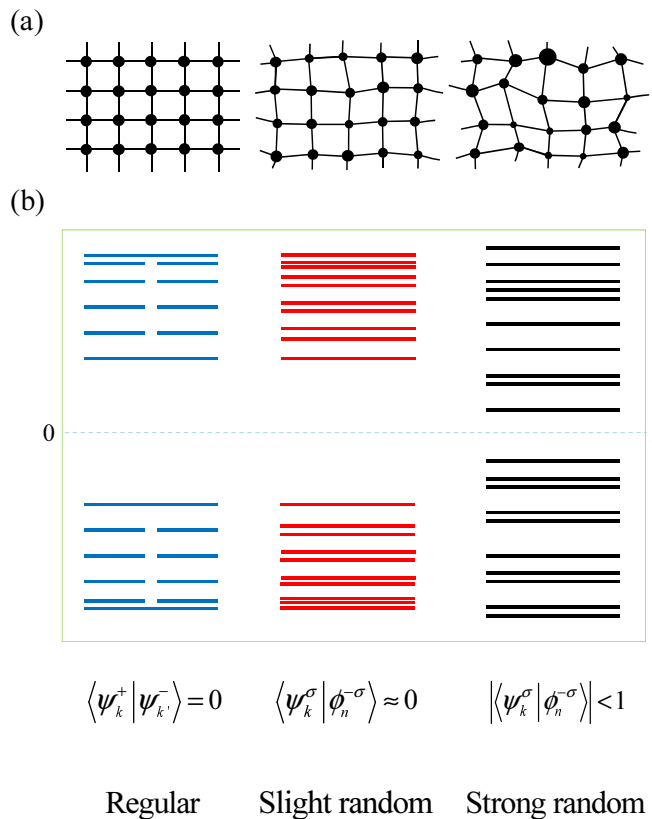


FIG. 1. (Color online) Schematic illustration of the concept of quasi-closed mappings. (a) Schematics of lattice systems with different imperfections: regular lattice with translational symmetry, noncrystalline lattices arising from slight and strong random parameters. (b) The corresponding spectra and the implication of perfect invariant sub-space (left) and quasi-closed mapping (middle). Slight disorder may destroy the degeneracy in the left spectrum but maintains structure of spectrum approximately, while in the right spectrum, strong disorder hybridizes the energy levels between upper and lower bands of the original system.

Hamiltonian is

$$H(t) = - \sum_{j=1}^{2N} [1 + (-1)^j \delta_j(t)] c_j^\dagger c_{j+1} + \text{H.c.} + \sum_{j=1}^{2N} (-1)^j V_j(t) c_j^\dagger c_j, \quad (6)$$

where particle operator obeys periodic boundary condition $c_{2N+1} = c_1$. Parameters $\{\delta_j(t)\}$ and $\{V_j(t)\}$ are two sets of time- and position-dependent numbers. In the following, we first establish the relation between the topological quantities, Zak phase and pumping charge, and the correlation functions. Subsequently, we investigate the influence of disorder perturbation on the corresponding correlation functions numerically.

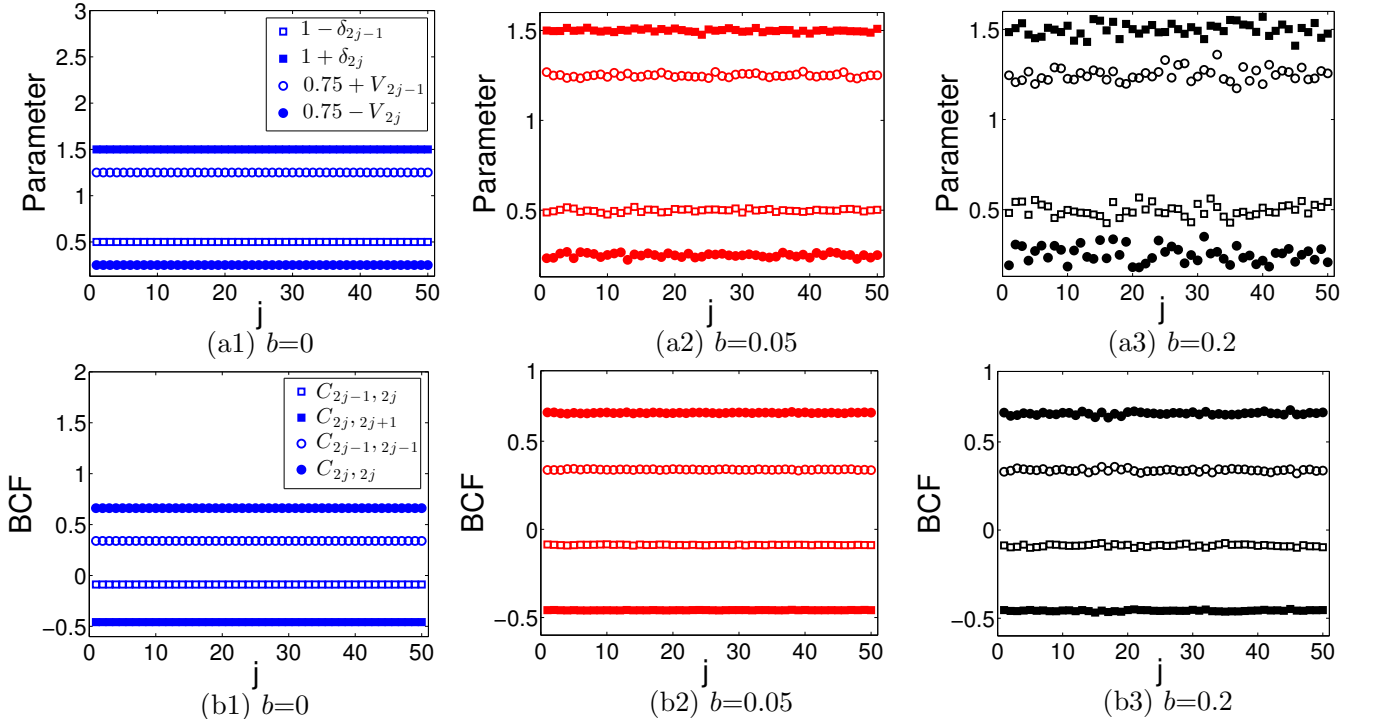


FIG. 2. (Color online) Numerical simulations for RM models with different strength of random parameters $(-b, b)$. (a1-a3) Plots of the hopping constant and on-site potential distributions along the chain for three typical random strengths. (b1-b3) Plots of the corresponding BCFs. The system parameters are $N = 50$, $V = 0.5$, and $\delta = 0.5$. The small random $b = 0.05$ almost does not affect the uniform distribution of four types of BCFs. Surprisingly, as b increases to 0.2, the induced fluctuations in (b3) are not so much in comparison with that in (a3).

A. Regular RM model

In the absence of the disorder, the Hamiltonian becomes $H_0(t)$ by taking $\delta_j = \delta(t)$ and $V_j = V(t)$. Before proceeding, we briefly recall the solution of H_0 , which reads

$$H_0 = - \sum_{j=1}^{2N} [1 + (-1)^j \delta] c_j^\dagger c_{j+1} + \text{H.c.} + V \sum_{j=1}^{2N} (-1)^j c_j^\dagger c_j. \quad (7)$$

It can be obtained by introducing linear transformation

$$\begin{cases} \alpha_k = N^{-1/2} \sum_{j=1}^N e^{-ikj} (e^{i\phi} \sin \frac{\theta}{2} c_{2j-1} - \cos \frac{\theta}{2} c_{2j}) \\ \beta_k = N^{-1/2} \sum_{j=1}^N e^{-ikj} (e^{i\phi} \cos \frac{\theta}{2} c_{2j-1} + \sin \frac{\theta}{2} c_{2j}) \end{cases}, \quad (8)$$

where the k -dependent parameters are defined by

$$\tan \phi = \frac{(1 + \delta) \sin k}{(1 - \delta) + (1 + \delta) \cos k}, \quad \tan \theta = \frac{|\gamma_k|}{-V}. \quad (9)$$

Based on this, we have the diagonal form of the Hamiltonian

$$H_0 = \sum_k \varepsilon_k (\alpha_k^\dagger \alpha_k - \beta_k^\dagger \beta_k), \quad (10)$$

where the spectrum

$$\varepsilon_k = \sqrt{V^2 + |\gamma_k|^2}, \quad (11)$$

with $\gamma_k = (1 - \delta) + (1 + \delta)e^{ik}$ and the momentum $k = 2n\pi/N$, $n = 1, 2, \dots, N$. The single-particle eigenvectors are $|\psi_k^+\rangle = \alpha_k^\dagger |0\rangle$ and $|\psi_k^-\rangle = \beta_k^\dagger |0\rangle$. In the following, we focus on the lower band by taking $|\psi_k\rangle = |\psi_k^-\rangle$, the result for upper band can be obtained directly.

The Zak phase as a related topological quantity can be expressed as

$$\mathcal{Z} = \frac{i}{2\pi} \int_{-\pi}^{\pi} \langle \psi_k | \partial_k | \psi_k \rangle dk = \mathcal{Z}_{\text{ad}} + \mathcal{Z}_{\text{com}}, \quad (12)$$

where \mathcal{Z}_{ad} attributes to adiabatic current and \mathcal{Z}_{com} arises from the center of mass. Here we would like to express them in term of the correlation functions

$$\mathcal{Z}_{\text{ad}} = \frac{N}{2\pi} \int \langle \psi_k | c_{2j-1}^\dagger c_{2j-1} | \psi_k \rangle d\phi - \frac{iN}{4\pi} \times \int \langle \psi_k | (e^{-i\phi} c_{2j-1}^\dagger c_{2j} - e^{i(\phi-k)} c_{2j}^\dagger c_{2j+1}) | \psi_k \rangle d\theta, \quad (13)$$

and

$$\mathcal{Z}_{\text{com}} = M_c = \sum_{j=1}^N j m_j, \quad (14)$$

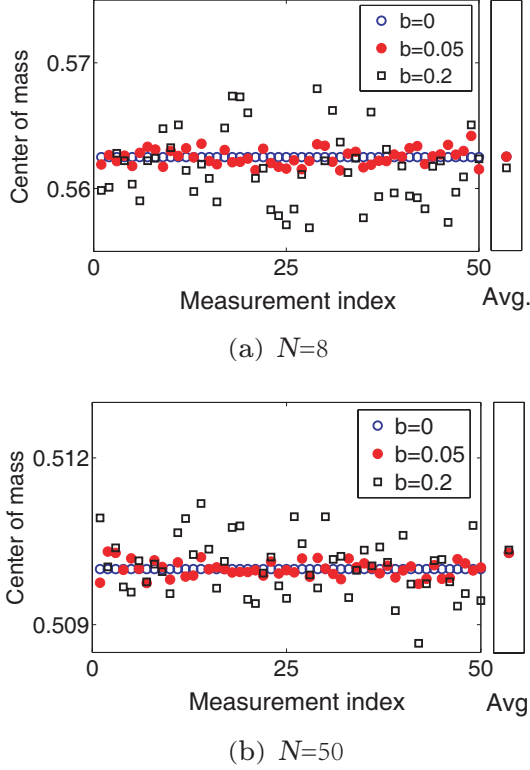


FIG. 3. (Color online) Plot of \mathcal{M}_c (left panels) defined in Eq. (22) for disordered RM model with a sequence of random number indicated by measurement index. The simulation is performed for different random strengths with $b = 0$ (empty blue circle), $b = 0.05$ (solid red circle) and $b = 0.2$ (empty black square). The average of \mathcal{M}_c (right panels) over 50 times measurement shows that the robustness of the center of mass for relatively large b value. The length of the ring (a) $N = 8$, (b) $N = 50$ and the parameters are $V = 0.5$, $\delta = 0.5$. Note that (a) and (b) are plotted in different scales, indicating that the fluctuation of \mathcal{M}_c decreases as N increases. In both cases, the average of \mathcal{M}_c are very close to that of zero b .

where the weight at j th site

$$m_j = \frac{1}{2N\pi} \int_{-\pi}^{\pi} \langle \psi_k | (c_{2j-1}^\dagger c_{2j-1} + c_{2j}^\dagger c_{2j}) | \psi_k \rangle dk. \quad (15)$$

It indicates that the correlations $\langle \psi_k | c_j^\dagger c_j | \psi_k \rangle$ and $\langle \psi_k | c_j^\dagger c_{j+1} | \psi_k \rangle$ have intimate connection with the Zak phase \mathcal{Z} .

Based on the the relations

$$\begin{cases} \langle \psi_k | c_{2j-1}^\dagger c_{2j-1} | \psi_k \rangle = N^{-1} \cos^2(\frac{\theta}{2}) \\ \langle \psi_k | c_{2j}^\dagger c_{2j} | \psi_k \rangle = N^{-1} \sin^2(\frac{\theta}{2}) \\ \langle \psi_k | c_{2j-1}^\dagger c_{2j} | \psi_k \rangle = \frac{1}{2} N^{-1} \sin \theta e^{i\phi} \\ \langle \psi_k | c_{2j}^\dagger c_{2j+1} | \psi_k \rangle = \frac{1}{2} N^{-1} \sin \theta e^{i(k-\phi)} \end{cases}, \quad (16)$$

we obtain the compact expressions

$$\mathcal{Z}_{\text{ad}} = \frac{1}{2\pi} \int_{\phi} \cos^2(\frac{\theta}{2}) d\phi \quad (17)$$

and

$$\mathcal{Z}_{\text{com}} = (N + 1)/(2N). \quad (18)$$

The constancy of \mathcal{Z} allows

$$d\mathcal{Z} = -\frac{1}{2\pi} \int_{\phi} \Omega_{\theta\phi} d\phi d\theta = J dt, \quad (19)$$

where $\Omega_{\theta\phi} = \frac{1}{2} \sin \theta$ is Berry curvature and

$$J = \frac{i}{2\pi} \int_{-\pi}^{\pi} [(\partial_t \langle \psi_k |) \partial_k | \psi_k \rangle - (\partial_k \langle \psi_k |) \partial_t | \psi_k \rangle] dk \quad (20)$$

is current across two neighboring sites. For a loop with

$$\delta(t + T) = \delta(t), V(t + T) = V(t) \quad (21)$$

around the point $\delta_c = V_c = 0$, the pumping charge $Q = \int_0^T J dt = \pm 1$ as a demonstration of Chern number. It is presumably that as a local quantity, Q should not change drastically in the presence of perturbation and takes the value around the original integral. This may be in accordance with the robustness of BCFs, which will be investigated numerically in the following section.

B. Disorder perturbation

In the presence of disorder, the definition of Zak phase is undefined due to the translational symmetry breaking. However, the concept of pumping charge is independent of the translational symmetry. It turns out that one of two ingredients of the pumping charge is the center of mass, which may not be a constant in the presence of disorder perturbation. In this section, we investigate the influence of disorder on the center of mass. In general, the center of mass for a energy band is defined as

$$\mathcal{M}_c = N^{-2} \sum_{n,j=1}^N j \langle \phi_n | (c_{2j-1}^\dagger c_{2j-1} + c_{2j}^\dagger c_{2j}) | \phi_n \rangle, \quad (22)$$

where $\{|\phi_n\rangle\}$ is the eigenstate of H in Eq. (6). When the perturbation switches on, i.e., $\delta_j \neq \delta$ and $V_j \neq V$, the translational symmetry is broken. However, according to our analysis in section II, the BCFs $C_{i,j} = \sum_n \langle \phi_n | c_i^\dagger c_j | \phi_n \rangle$ are still robust if the band gap does not collapse and we can have a conclusion with

$$\begin{aligned} & \sum_n \langle \phi_n | (c_{2j-1}^\dagger c_{2j-1} + c_{2j}^\dagger c_{2j}) | \phi_n \rangle \\ & \approx \sum_k \langle \psi_k | (c_{2j-1}^\dagger c_{2j-1} + c_{2j}^\dagger c_{2j}) | \psi_k \rangle = 1. \end{aligned} \quad (23)$$

Then \mathcal{M}_c is approximately a constant in the presence of disorder. To demonstrate this point and find the extent to which the deviation of $C_{i,j}$ is negligible, we numerically compute $C_{i,i}$ and $C_{i,i+1}$ for disorder RM model, in which

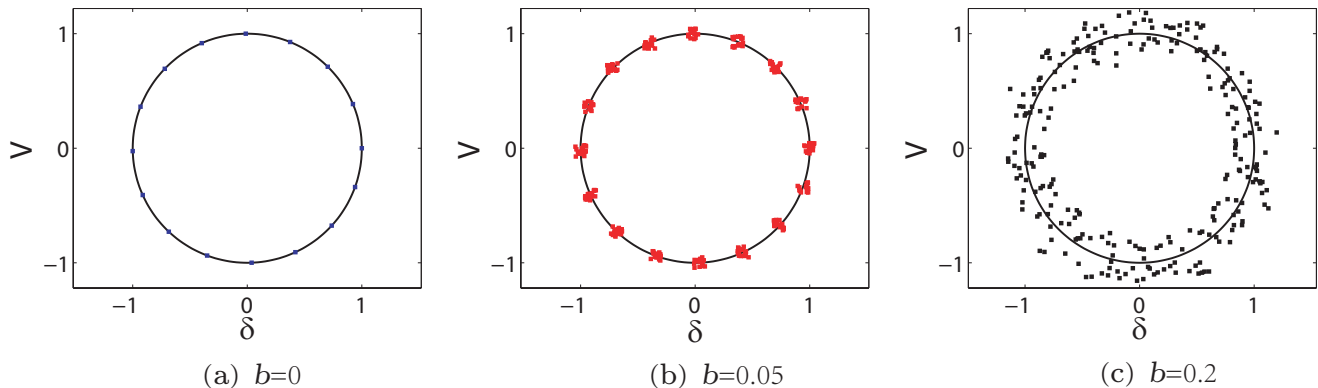


FIG. 4. (Color online) Plots of $\{\delta_j(t_l), V_j(t_l)\}$ in V - δ plane from Eq. (27) with (a) $b = 0$, (b) $b = 0.05$, and (c) $b = 0.2$. Here we take $\delta_0 = V_0 = 0$, $R = 1$, $M = 16$ and $N = 8$. The corresponding discretized time is $t_l = 2\pi(l + 1)/(16\omega)$ with $l = 0, 1, \dots, 15$.

$\{\delta_j\}$ and $\{V_j\}$ are two sets of random numbers around δ and V , respectively. Actually, $C_{i,i}$ and $C_{i,i+1}$ are immune to the random perturbation no matter $\{\delta_j\}$ and $\{V_j\}$ are real or imaginary. For clarity, we only consider the real random numbers in later discussions.

Numerical simulation is performed by taking two sets of random numbers $\{\delta_j\}$ and $\{V_j\}$ around δ and V . The random number parameter can be taken as

$$\delta_j = \delta + \text{ran}(-b, b), V_j = V + \text{ran}(-b, b), \quad (24)$$

where $\text{ran}(-b, b)$ denotes a uniform random number within $(-b, b)$. In Fig. 2, we plot the results with several typical values of b . We find that $C_{i,i}$ and $C_{i,i+1}$ are still immune to the random perturbation for relatively large b value. This will result in the robustness of \mathcal{M}_c against the disorder. To estimate the effect of disorder, the fluctuation of \mathcal{M}_c , we plot the center of mass with several typical values of b in Fig. 3. It shows that the fluctuation of \mathcal{M}_c is within 0.1% for large size system. The result indicates that although the translational symmetry is broken, the center of mass is still time-independent approximately, contributing much less to the current or pumping charge. It is expected that the pumping charge can still take the role of topological invariant.

IV. ROBUSTNESS OF PUMPING CHARGE

In this section, we focus on the Thouless quantum pump in the disorder system. Inspired by the above analysis, we expect that there exists residual topological feature in the disordered RM model, which may be unveiled by the pumping charge. Numerical simulation is performed by taking

$$\begin{aligned} \delta_j(t) &= \delta_0 + R \cos(\omega t) + \text{ran}(-b, b)_t, \\ V_j(t) &= V_0 + R \sin(\omega t) + \text{ran}(-b, b)_t, \end{aligned} \quad (25)$$

where the subscript index t indicates the random number is time dependent. The computation is performed by us-

ing a uniform mesh in the time discretization. The time evolution is a little different from the previous works, where parameters vary smoothly in time. This is implemented by discretizing the time t into t_i , with $t_0 = 0$ and $t_M = T$. For a given initial eigenstate $|\phi_n(0)\rangle$, the time evolved state is computed by

$$|\phi_n(t_l)\rangle = \prod_{l=1}^M \exp[-iH(t_{l-1})(t_l - t_{l-1})] |\phi_n(0)\rangle, \quad (26)$$

where each $H(t_l)$ corresponds to a set of random number $\text{ran}(-b, b)$. In this work, the parameters for $H(t_l)$ is taken in the form

$$\begin{aligned} \delta_j(t_l) &= \delta_0 + R \cos(\omega t_l) + \text{ran}(-b, b)_l, \\ V_j(t_l) &= V_0 + R \sin(\omega t_l) + \text{ran}(-b, b)_l, \end{aligned} \quad (27)$$

with $l \in [0, M - 1]$. In Fig. 4, we illustrate this scheme by plotting $\{\delta_j(t_l), V_j(t_l)\}$ with several typical b but a small M and N . In the simulation, the number of M is taken to be sufficient large in order to get convergent result. The total pumping charge passing the site j attributed from all channels of lower energy band during the time evolution period T , can be expressed as

$$\begin{aligned} Q &= \sum_{n=1}^N \int_0^T \langle \phi_n(t) | \mathcal{J}_j | \phi_n(t) \rangle dt \\ &\approx \sum_{n=1}^N \sum_{l=1}^M \langle \phi_n(t_l) | \mathcal{J}_j | \phi_n(t_l) \rangle (t_l - t_{l-1}), \end{aligned} \quad (28)$$

which is independent of j for an adiabatic circle. Here the current operator is

$$\mathcal{J}_j = \frac{1}{i} \left\{ \begin{array}{l} (1 - \delta_j) |j\rangle \langle j+1| - \text{H.c.}, (j = 2m - 1) \\ (1 + \delta_j) |j\rangle \langle j+1| - \text{H.c.}, (j = 2m) \end{array} \right\}, \quad (29)$$

where $m = 1, 2, \dots, N$. Fig. 5 and Fig. 6 plot the simulations of particle current and the corresponding total probability for several typical cases, in order to see to

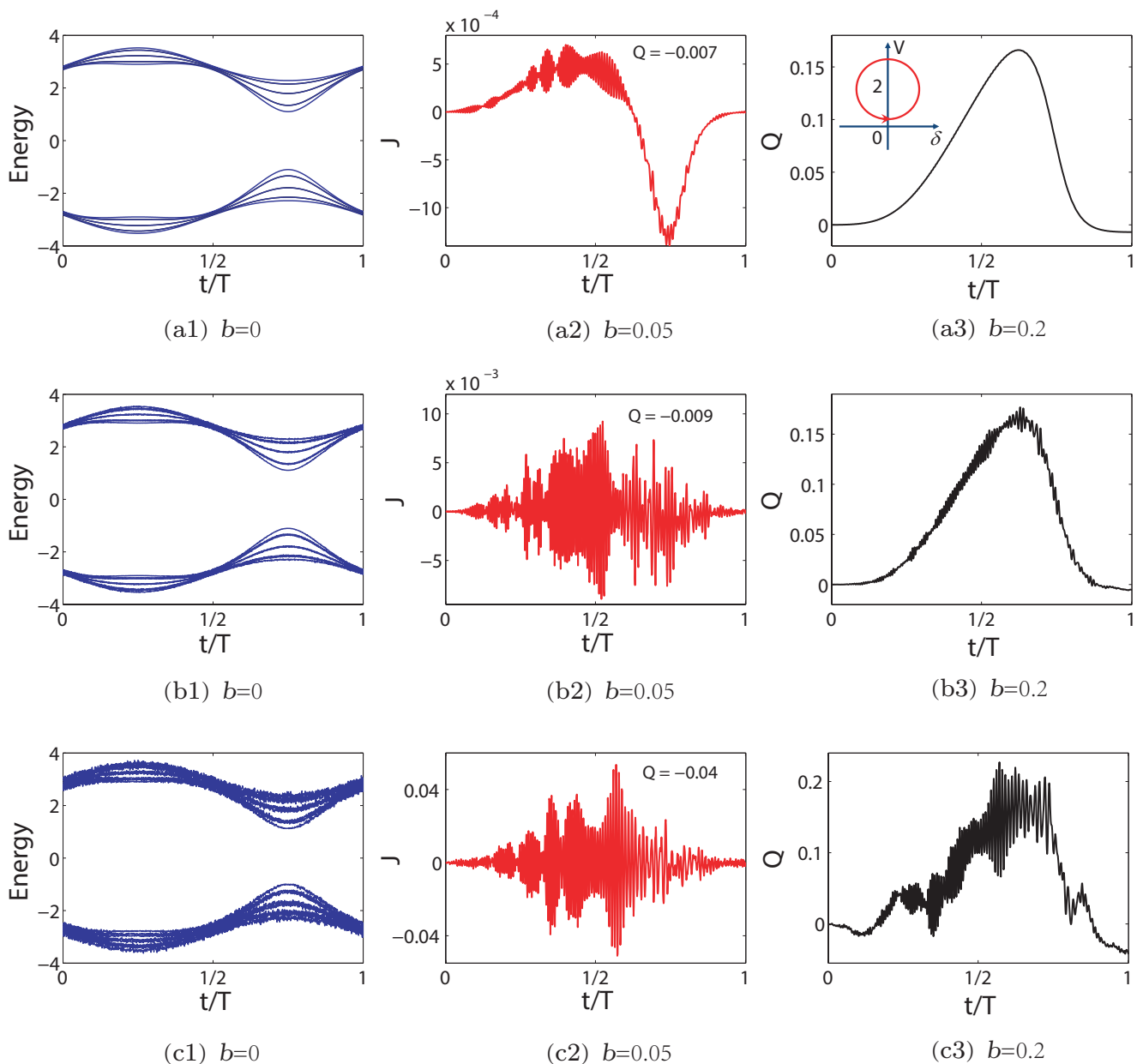


FIG. 5. (Color online) Numerical simulations of time evolution driven by the time-dependent Hamiltonian with parameters in Eq. (27). Plots of the instantaneous spectra (a1-c1) local current (a2-c2) and charge accumulation (a3-c3) as function of evolution time for several typical random strengths b . The parameters are taken as $(\delta_0, V_0) = (0, 2)$, $R = 1$, $N = 8$, $\omega = 6 \times 10^{-5}$, and $M = 5 \times 10^4$. We note that the loop of time evolution does not enclose the degeneracy point $(0, 0)$. The obtained pumping charges are very close zero, even for $b = 0.2$, indicating the robustness of the pumping charge.

what extent the pumping charge can be regarded as a quasi topological invariant. Fig. 7 plots the pumping charges for different loops and random strengths. It indicates that weak disorder cannot affect the quantization of the pumping charge, and in the case with strong disorder, pumping charge can still identify the transition point approximately. As the size of the system increases, the influence of disorder becomes weak. It shows that the pumping charge is a reliable quantity to measure the topological invariant in experiment. Our finding indi-

cates that the topological feature may also emerge in a noncrystalline system in an approximate manner.

V. SUMMARY

In summary, we have analyzed the insensitivity of a topological invariant to a disorder perturbation. In general, we find that there are a kinds of quantities, such as BCFs, which are robust against the disorder. The under-

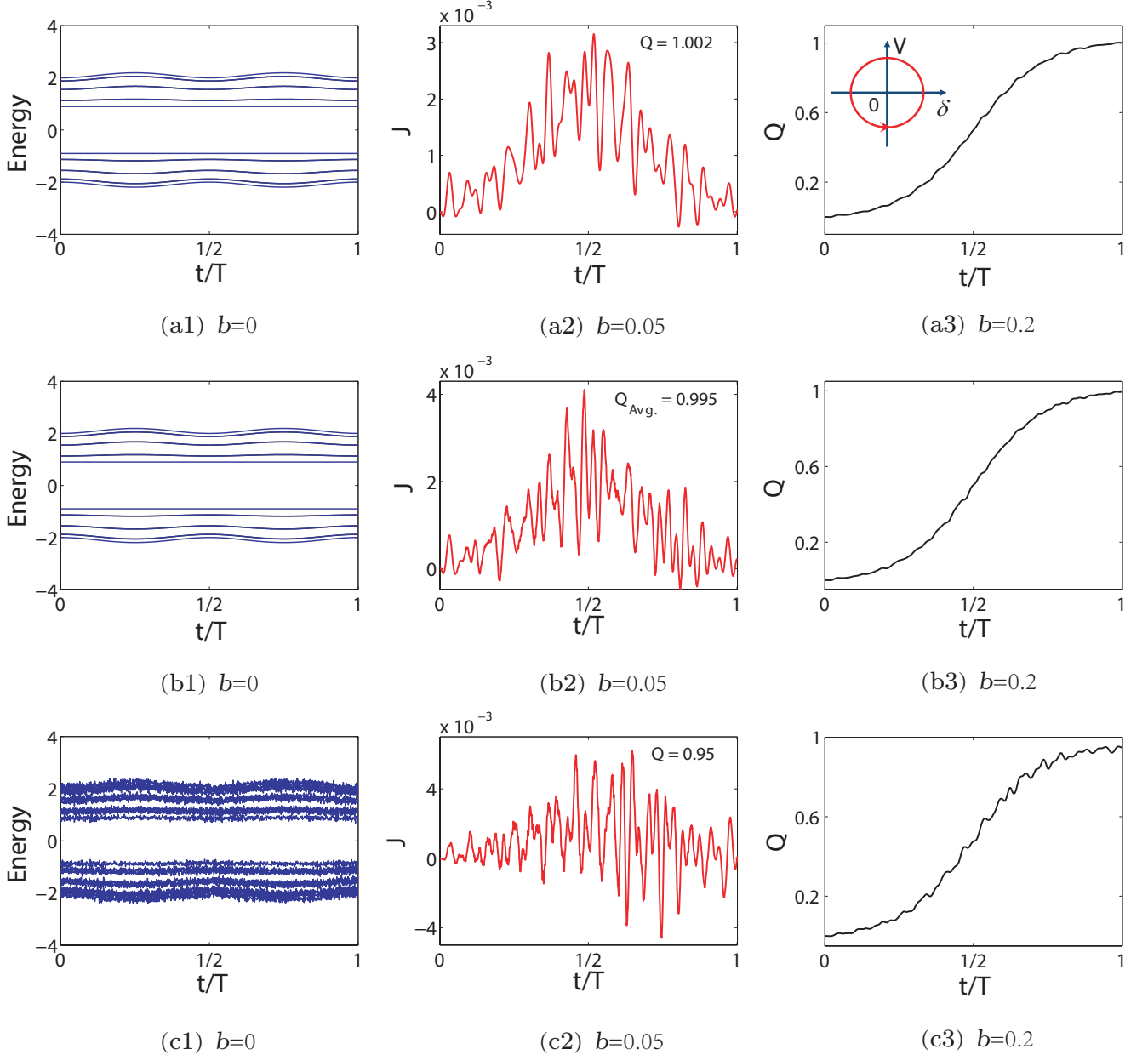


FIG. 6. (Color online) The same as Fig. 5 but for $(\delta_0, V_0) = (0, 0)$. The loop of time evolution encloses the degeneracy point $(0, 0)$. The obtained pumping charges is very close to 1 for $b = 0.05$, indicating the robustness of the pumping charge. In the case with $b = 0.2$, the pumping charge is close to 1 with 5% deviation.

lying mechanism is that the weak disorder cannot destroy the energy band structure although it breaks the translational symmetry. This manifests that a noncrystalline system may be topologically nontrivial in an approximate manner, since an approximate topological invariant can be retrieved. We have demonstrated this point by a time-dependent disordered RM model. We computed the dynamical topological invariant by accumulating the measurable local current without the requirement of translational symmetry. The results indicate that (i) weak disorder almost has no effect on the integer of Chern

number; (ii) as disorder increases, the quasi Chern number deviates from integer, but is still evidently to characterize the phase transition. Our finding provides a way of extracting topological invariant from imperfect system and predicts the existence of quasi topological phase.

ACKNOWLEDGMENTS

We acknowledge the support of National Natural Science Foundation of China (Grant No. 11874225).

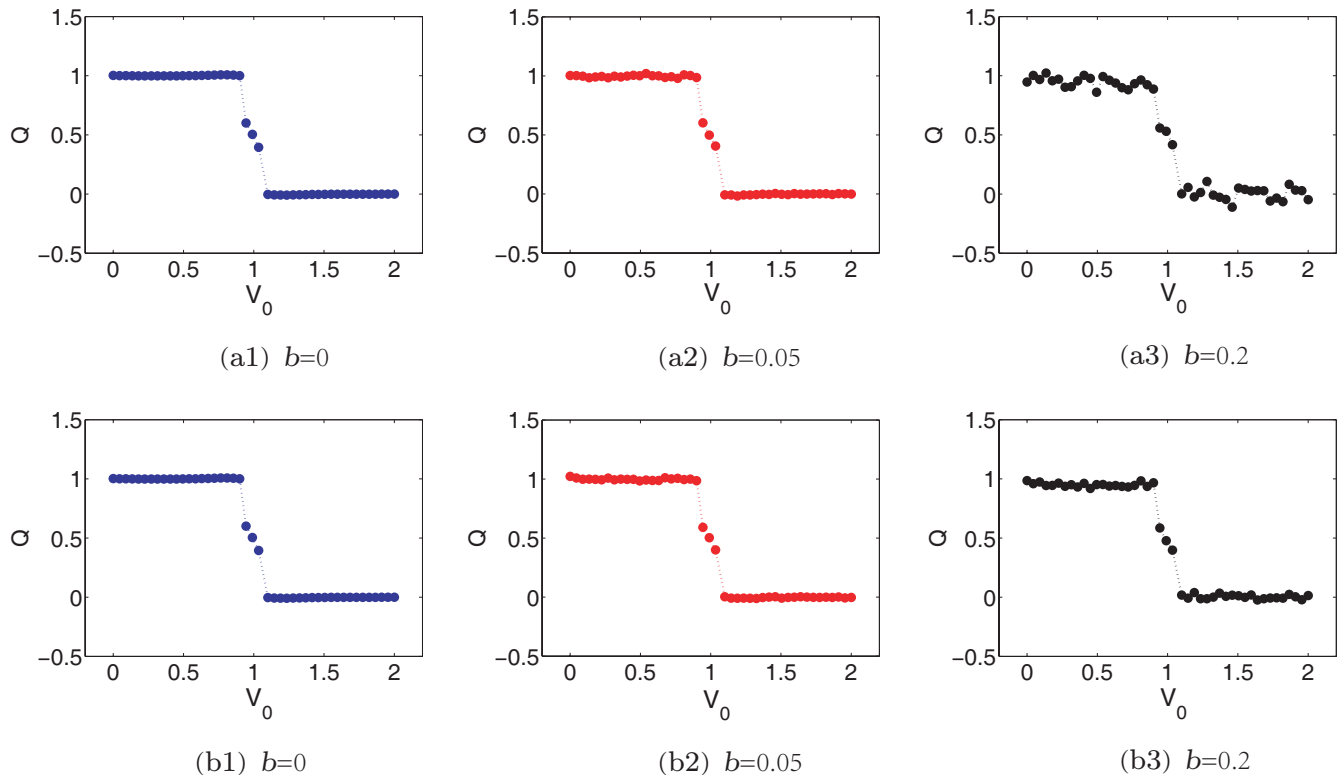


FIG. 7. (Color online) Plots of the pumping charge as function of the position $(\delta_0, V_0) = (0, V_0)$, obtained by numerical simulations as the same in Fig. 5 and Fig. 6 for systems with (a1-a3) $N = 8$, (b1-b3) $N = 50$. It indicates that Q experiences evident jump at the critical point, even for relatively large random strength $b = 0.2$. Large N can increase the robustness of Q against the disorder, supporting the concept of topological invariant in an approximate manner.

* songtc@nankai.edu.cn

- ¹ D. J. Thouless, M. Kohmoto, M. P. Nightingale, and M. den Nijs, Quantized Hall Conductance in a Two-Dimensional Periodic Potential, *Phys. Rev. Lett* **49**, 405 (1982).
- ² A Yu Kitaev, Unpaired Majorana fermions in quantum wires, *Phys. Usp.* **44**, 131 (2001).
- ³ Shinsei Ryu and Yasuhiro Hatsugai, Topological Origin of Zero-Energy Edge States in Particle-Hole Symmetric Systems, *Phys. Rev. Lett.* **89**, 077002 (2002).
- ⁴ Markus Greiner, Olaf Mandel, Tilm Esslinger, Theodor W. Hänsch, and Immanuel Bloch, Quantum phase transition from a superfluid to a Mott insulator in a gas of ultracold atoms. *Nature* **415**, 39-44 (2002).
- ⁵ Shuichi Murakami, Naoto Nagaosa, and Shou-Cheng Zhang, Spin-hall insulator, *Phys. Rev. Lett.* **93**, 156804 (2004).
- ⁶ C. L. Kane and E. J. Mele, Quantum Spin Hall Effect in Graphene, *Phys. Rev. Lett.* **95**, 226801 (2005).
- ⁷ B. Andrei Bernevig, Taylor L. Hughes, and Shou-Cheng Zhang, Quantum spin Hall effect and topological phase transition in HgTe quantum wells, *Science* **314**, 1757-1761 (2006).
- ⁸ Liang Fu and C. L. Kane, Topological insulators with inversion symmetry, *Phys. Rev. B* **76**, 045302 (2007).

- ⁹ Liang Fu, C. L. Kane, and E. J. Mele, Topological Insulators in Three Dimensions, *Phys. Rev. Lett.* **98**, 106803 (2007).
- ¹⁰ Andreas P. Schnyder, Shinsei Ryu, Akira Furusaki, and Andreas W. W. Ludwig, Classification of topological insulators and superconductors in three spatial dimensions, *Phys. Rev. B* **78**, 195125 (2008).
- ¹¹ Shinsei Ryu, Andreas P Schnyder, Akira Furusaki, and Andreas W W Ludwig, Topological insulators and superconductors: tenfold way and dimensional hierarchy, *New J. Phys.* **12**, 065010 (2010).
- ¹² M. Z. Hasan and C. L. Kane, *Colloquium*: Topological insulators, *Rev. Mod. Phys.* **82**, 3045 (2010).
- ¹³ Gang Xu, Hongming Weng, Zhijun Wang, Xi Dai, and Zhong Fang, Chern Semimetal and the Quantized Anomalous Hall Effect in HgCr₂Se₄, *Phys. Rev. Lett.* **107**, 186806 (2011).
- ¹⁴ A. A. Burkov and Leon Balents, Weyl semimetal in a topological insulator multilayer, *Phys. Rev. Lett.* **107**, 127205 (2011).
- ¹⁵ Xiao-Liang Qi and Shou-Cheng Zhang, Topological insulators and superconductors, *Rev. Mod. Phys.* **83**, 1057 (2011).
- ¹⁶ S. M. Young, S. Zaheer, J. C. Y. Teo, C. L. Kane, E. J. Mele, and A. M. Rappe, Dirac Semimetal in Three Dimen-

- sions, *Phys. Rev. Lett.* **108**, 140405 (2012).
- ¹⁷ Zhijun Wang, Yan Sun, Xing-Qiu Chen, Cesare Franchini, Gang Xu, Hongming Weng, Xi Dai, and Zhong Fang, Dirac semimetal and topological phase transitions in A_3Bi ($A=Na, K, Rb$), *Phys. Rev. B* **85**, 195320 (2012).
 - ¹⁸ C.-E. Bardyn, M. A. Baranov, E. Rico, A. İmamoğlu, P. Zoller, and S. Diehl, Majorana modes in driven-dissipative atomic superfluids with a zero Chern number, *Phys. Rev. Lett.* **109**, 130402 (2012).
 - ¹⁹ Leticia Tarruell, Daniel Greif, Thomas Uehlinger, Gregor Jotzu, and Tilman Esslinger, Creating, moving and merging Dirac points with a Fermi gas in a tunable honeycomb lattice, *Nature* **483**, 302-305 (2012).
 - ²⁰ Zhijun Wang, Hongming Weng, Quansheng Wu, Xi Dai, and Zhong Fang, Three-dimensional Dirac semimetal and quantum transport in Cd_3As_2 , *Phys. Rev. B* **88**, 125427 (2013).
 - ²¹ Z. K. Liu, B. Zhou, Y. Zhang, Z. J. Wang, H. M. Weng, D. Prabhakaran, S.-K. Mo, Z. X. Shen, Z. Fang, X. Dai, Z. Hussain, and Y. L. Chen, Discovery of a Three-Dimensional Topological Dirac Semimetal, Na_3Bi , *Science* **343**, 864-867 (2014).
 - ²² Meng Xiao, Guan cong Ma, Zhiyu Yang, Ping Sheng, Z. Q. Zhang, and C. T. Chan, Geometric phase and band inversion in periodic acoustic systems, *Nat. Phys.* **11**, 240-244 (2015).
 - ²³ Hongming Weng, Chen Fang, Zhong Fang, B. Andrei Bernevig, and Xi Dai, Weyl Semimetal Phase in Non-centrosymmetric Transition-Metal Monophosphides, *Phys. Rev. X* **5**, 011029 (2015).
 - ²⁴ Ling Lu, Zhiyu Wang, Dexin Ye, Lixin Ran, Liang Fu, John D. Joannopoulos, and M. Soljačić, Experimental observation of Weyl points, *Science*, **349**, 622-624 (2015).
 - ²⁵ Daniel Leykam, M.C. Rechtsman, and Y.D. Chong, Anomalous Topological Phases and Unpaired Dirac Cones in Photonic Floquet Topological Insulators, *Phys. Rev. Lett.* **117**, 013902 (2016).
 - ²⁶ Ching-Kai Chiu, Jeffrey C.Y. Teo, Andreas P. Schnyder, and Shinsei Ryu, Classification of topological quantum matter with symmetries, *Rev. Mod. Phys.* **88**, 035005 (2016).
 - ²⁷ Flore K. Kunst, Guido van Miert, and Emil J. Bergholtz, Lattice models with exactly solvable topological hinge and corner states, *Phys. Rev. B* **97**, 241405(R) (2018).
 - ²⁸ N. P. Armitage, E. J. Mele, and Ashvin Vishwanath, Weyl and Dirac semimetals in three-dimensional solids, *Rev. Mod. Phys.* **90**, 015001 (2018).
 - ²⁹ I. C. Fulga, B. van Heck, J. M. Edge, and A. R. Akhmerov, Statistical topological insulators, *Phys. Rev. B* **89**, 155424 (2014).
 - ³⁰ Zohar Ringel, Yaacov E. Kraus, and Ady Stern, Strong side of weak topological insulators, *Phys. Rev. B* **86**, 045102 (2012).
 - ³¹ Adhip Agarwala and Vijay B. Shenoy, Topological Insulators in Amorphous Systems, *Phys. Rev. Lett.* **118**, 236402 (2017).
 - ³² D. J. Thouless, Quantization of particle transport, *Phys. Rev. B* **27**, 6083 (1983).
 - ³³ Y. Hatsugai, and T. Fukui, Bulk-edge correspondence in topological pumping, *Phys. Rev. B* **94**, 041102(R) (2016).
 - ³⁴ Di Xiao, Ming-Che Chang, and Qian Niu, Berry phase effects on electronic properties, *Rev. Mod. Phys.* **82**, 1959 (2010).
 - ³⁵ R. Wang, C. Li, X. Z. Zhang, and Z. Song, Dynamical bulk-edge correspondence for degeneracy lines in parameter space, *Phys. Rev. B* **98**, 014303 (2018).
 - ³⁶ R. Wang, X. Z. Zhang, and Z. Song, Dynamical topological invariant for the non-Hermitian Rice-Mele model, *Phys. Rev. A* **98**, 042120 (2018).
 - ³⁷ Marcos Atala, Monika Aidelsburger, Julio T. Barreiro, Dmitry Abanin, Takuya Kitagawa, Eugene Demler, and Immanuel Bloch, Direct measurement of the Zak phase in topological Bloch bands, *Nat. Phys.* **9**, 795-800 (2013).